Laterally Loaded Cast-in-Drilled-Hole Piles

C. K. SHEN, S. BANG, M. DESALVATORE, AND C. J. PORAN

The behavior of cast-in-drilled-hole pile has been investigated in detail with an instrumented model test pile embedded in either level or sloping ground of sand or silty clay soil. Upslope and downslope as well as parallel directional lateral loads were applied to the model test pile to measure the lateral resistance and the load-deflection relationship. Parameters such as the embedment length, the slope of the ground, the distance from the edge of the slope, and the cyclic loading were included in the study.

A large number of subsurface structures are designed mainly to resist the lateral or overturning loads applied above the ground level. These subsurface structures derive their bearing capacity from the passive earth resistance against lateral movements (translation or rotation). One of the widely used types of foundation in this category is the cast-in-drilled-hole (CIDH) pile. Piles of this type are normally less than 12 ft long and have a length-to-diameter ratio ranging from 2 to 1 for short piles to about 10 for longer piles. Because of their relatively low slenderness ratios and high rigidity with respect to the surrounding soils, they are conventionally considered as rigid members in design and analysis. Structures supported by CIDH piles are numerous, notably posts for large road and commercial signs and sound barrier walls for noise control along urban freeways.

A comprehensive investigation conducted more than 15 years ago by the Texas Department of Highways (*1–3*) concluded that the conventional design of CIDH piles appeared to be conservative. This study proposed a rigorous but simple-to-use alternative design method for calculating ultimate lateral loads. The formulation includes the development of shear stresses and the circumferential variation of normal stresses around a pile. The formulation, however, does not completely satisfy all the stress boundary conditions and the failure criterion; most importantly it does not include a provision for sloping ground conditions. In practice, for instance, sound barrier walls are frequently placed near the edge of roadway embankments. In light of the above, there appears to be a need to conduct a study to evaluate the lateral resistance of CIDH piles placed in level or sloping ground with the final objective of establishing an improved design methodology as applied to highway-related structures.

C. K. Shen, Department of Civil Engineering, University of California, Davis, Calif. 95616. S. Bang, Department of Civil Engineering, South Dakota School of Mines and Technology, Rapid City, S. Dak. 57701-3995. M. DeSalvatore, Geotechnical Branch, California Department of Transportation Laboratory, 5900 Folsom Boulevard, Sacramento, Calif. 95819. C. J. Poran, Department of Civil Engineering, Polytechnique Institute of New York, Brooklyn, N.Y. 11201.

LITERATURE REVIEW

The usual approach to treat the problem of a laterally loaded pile is first to categorize the pile as either rigid or flexible. A clear distinction between those two, however, does not exist. It has been suggested that the rigidity of a pile can be related to the ratio of the flexural stiffness of the pile and the foundation soil modulus. Taking into consideration a wide range of soil stiffness, Kasch et al. (*4*) concluded that in order to ensure rigid pile behavior, the length-to-diameter ratio of a pile should not exceed about 6, but could be as high as 10 under certain conditions, such as in weak soils; also that a ratio of 20 or more ensures flexible pile behavior. Accordingly, the CIDH pile can be considered as a relatively rigid pile.

One of the first attempts to calculate the ultimate lateral resistance of a short rigid pile in cohesionless soil was made by Broms (*5*). He assumed that the active earth pressure acting on the back of a pile is negligible, that the distribution of passive earth pressure along the front of a pile is equal to three times the Rankine's passive pressure, and that the shape of a pile section has no influence on the distribution of ultimate soil pressure.

Based on the equilibrium of a tetrahedron-shaped soil failure wedge under lateral load, Reese et al. (*6*) formulated the ultimate soil resistance for a short rigid pile. The total ultimate lateral resistance of the pile is equal to the passive force minus the active force. The active force is computed from Rankine's theory and the passive force from the geometry of the wedge with boundary forces following the Mohr-Coulomb failure criterion.

Broms (*7*) also developed a theory to calculate the ultimate lateral resistance of a short rigid pile in cohesive soil. He suggested a simplified lateral soil resistance distribution: zero from the ground surface to a depth of 1.5 times the pile diameter, and a constant value of 9 times the undrained shear strength below this depth.

Using a failure wedge similar to the one used in cohesionless soils, Reese (*8*) formulated an expression for the ultimate resistance of a laterally loaded pile in soft clay. The resulting ultimate resistance per unit length of pile consists of three terms. The first indicates the resistance at the ground surface, the second relates to the increase in resistance with depth resulting from overburden pressure, and the third is a geometrically related restraint term. Matlock (*9*) later found that the third term in Reese's expression did not agree with experimental observations and suggested an alternative expression.

Ivey (*1*) studied the ultimate resistance of drilled piles in level ground and proposed a comprehensive design method. In his approach, unlike the conventional ones, both normal and shear stresses acting on all faces of the pile were considered. Distributions of these stresses resulting from a rotation of the pile were assumed to vary along the circumferential direction by cosine and sine functions. The point of rotation and the resulting ultimate lateral resistance of the pile were then calculated from the equilibrium equations. The proposed method was later modified based on model test results (*3*). Although the theory includes most of the essential characteristics of rigid pile behavior under lateral loads, the application may be limited because (a) fully active and passive conditions based on Rankine's theory were used, (b) shear stresses did not totally satisfy the Mohr-Coulomb failure criterion, and (c) most of the test results used to verify the theory, particularly those in sands, were obtained from scaled model piles of limited range.

Other design methods available for short rigid piles are by Hays et al. (*10*), Ivey and Dunlap (*2*), Ivey and Hawkins (*11*), Davidson et al. (*12*), Lytton (*13*), Ivey et al. (*3*), Seiler (*14*), Hansen (*15*), and others. In general, the Ivey and Dunlap and the Ivey and Hawkins methods yield conservative values (*4*); whereas Hansen's and Lytton's methods yield consistently unconservative values for larger piles (*16*). Broms' method yields conservative results in stiff clays but unconservative results in soft clays (*16*).

There have also been many experimental studies on the load-deflection relationships (*2, 4, 10, 17, 18*) and the earth pressure measurements (*4, 16, 17, 19–21*) along laterally loaded rigid piles. In general the measured lateral earth pressure distributions are parabolic shaped. Based on the measured earth pressure distribution, Biershwale et al. (*16*) reported that the point of rotation or the point of zero lateral stress is located at approximately 0.7 times the embedment length of a pile as measured from the ground surface. This generally coincides with results reported by other studies (*1, 4, 10, 17, 19*) stating that the rotation point lies in the vicinity of two-thirds of the embedment length. However, studies (*2, 4, 10, 18, 22*) also indicated that the point of rotation does not remain at a constant depth below the ground surface, rather it moves to lower depths as the lateral load is increased. The point of rotation could also move upward if the strength of the soil decreases with depth (*2*). In general, the point of rotation shifts downward from some point below the middle of the embedded pile for lighter loads to a point approximately three-quarters of the embedment depth for maximum loads.

As indicated in this brief literature review, considerable research has been conducted on the ultimate soil resistance and pile capacity of laterally loaded piles. Most of the solutions, however, are based on the ultimate or limiting equilibrium conditions, and thus cannot be used to compute lateral earth pressures at conditions other than failure. In order to understand the soil-rigid pile interaction more clearly, a comprehensive investigation including a laboratory model study was conducted. Considerations were given to both the working stress and ultimate stress states in level and sloping ground. The pile model study is described in detail in this study.

MODEL TESTING

Testing Facility

The testing facility included a large test bin, an instrumented pile, a loading system, and a data-acquisition system. The wooden test bin (12 ft × 4 ft × 4 ft) was composed of ¾-in.-thick plywood sidewalls, two sets of perimeter steel box beams to reinforce the walls, and a plywood bottom. A 2024-T4 aluminum tube pipe 0.25 in. thick, and 40 in. long, with an outside diameter of 3.5 in., was selected to represent the model pile. To instrument the model pile, the pipe was cut into two half-circular sections with shear pins installed along both sides of one of the half pipe sections.

Eleven lateral pressure gauge mounts were installed in each of the two half pipe sections at a spacing of 3 in./mount. The large number of pressure gauge mounts allowed the locations of the pressure gauges to be changed from test to test. Finally, a thin coat of medium sand was glued to the outer surface of the model pile to produce the typical concrete-soil interface friction. Ten Kulite model KHM-375-series pressure gauges were installed in the gauge mounts along the front and back sides of the model pile, with the pressure-sensitive diaphragm placed flush with the surface of the model pile and in alignment with its length.

A set of electric circuit boards was designed and mounted inside the model pile to perform the multiplexing and signal-conditioning functions so that all the signals could be transmitted from the model pile to the data-acquisition system by a single set of wires. A picture of the fully instrumented model pile is shown in Figure 1.

An electrohydraulic closed-loop testing system was modified to apply the lateral load to the instrumented model pile. The hydraulic actuator was programmed to pull or push the

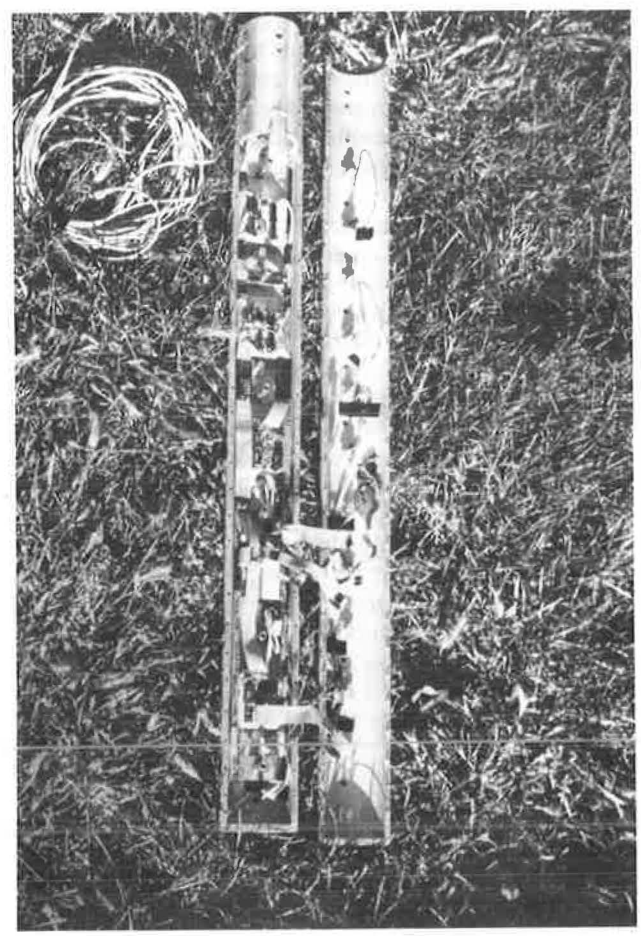

FIGURE 1 Model test pile with instrumentation.

TABLE 1 SOIL PROPERTIES

	Yolo Loam	Cache Creek Sand
Cohesion (psf)	1,800 - 2,750	0
Friction Angle	24° - 26°	40° - 43°
Maximum Dry Density (pcf) (Modified AASHTO Method T-180-57)	116	114.3
Liquid Limit	27	--
Plasticity Index	12	--
Water Content	15.3 - 17.4%	--
Unified Classification	CL	SP

model pile laterally at a rate of 0.2 in./min. A lateral displacement of 3 in. was applied to the top of the model pile that corresponds approximately to a 5° angular rotation assuming no tip movement.

The load applied to the model pile was measured by a load cell connected between the hydraulic actuator and the loading rod. The lateral displacement and angular rotation of the model pile were measured by two linear variable differential transformers (LVDTs) attached to the top of the pile. The angular rotation and lateral displacement (much less than 3 in.) at ground level were calculated from the difference between LVDT readings and the geometry of the setup. Movements of the LVDTs were monitored and recorded by the data-acquisition system.

A microcomputer-based data-acquisition system was used for recording and processing data. Signals from various sensors picked up by the signal conditioners were filtered, converted, and then channeled through a multiplexer to a digitally programmable amplifier-attenuator that adjusted the output signal level. The adjusted analog signals were then fed through an analog-to-digital converter that digitized the signals that were to be processed by the computer.

Testing Program

The model pile testing program required the construction of either level ground or sloping ground embankments made of pit-run, air-dried river sand or silty clay. For each type of the embankment material studies, parameters such as embankment geometry and loading direction were varied to evaluate the load-versus-displacement response of the pile-soil system and the corresponding measurements of lateral earth pressure distribution in longitudinal and circumferential directions.

The testing program involved a sequence of events composed of sample preparation, placement of pile, and testing and data collection. Locally available silty clay (Yolo Loam) and sand (Cache Creek sand) were chosen as embankment materials. Their pertinent properties are described in Table 1.

A brief description of cohesive soil sample preparation is given as follows. The bin was initially treated with a waterproofing seal to help retain moisture in the soil. For each lift of compaction, approximately 1,500 lb of soil was placed in the test bin to make a 4- to 5-in.-thick loose layer. The soil layer was then compacted, first with a vibratory plate compactor and then with a pneumatic hammer. A uniform amount of compaction effort was applied to each layer during compaction to achieve uniformity in shear strength and dry unit weight. The specification for compaction control of the cohesive soil was for each layer to be compacted at 3.5 percent above the optimum moisture content and to a minimum of 95 percent of the maximum dry density obtained by the modified AASHTO method T-180-57. Compaction was carried out on the wet side of optimum in an effort to avoid overcompaction of the layers.

When preparation of a soil sample was completed, damp burlap was placed on the surface of the soil sample and then the entire bin was covered with a sheet of plastic to prevent evaporation of moisture from the soil sample. In an effort to obtain a more uniform moisture content, the soil sample was permitted to sit covered overnight.

After allowing the soil sample to set overnight, a posthole driller was used to drill a 9-in. diameter hole to the desired depth in the embankment soil. The model test pile was then lowered into the hole, aligned vertically and then clamped into place. The material removed during drilling was broken up and placed back around the model pile in 1-in. layers and compacted with a slide hammer compactor.

The method of compaction used in cohesionless soil consisted of compacting 4- to 5-in.-thick loose layers of sand in the test bin with a vibratory sled. To place the test pile in the compacted sand, a vibratory-pneumatic driving system was developed. The pile was lowered into the embankment by a combined action of vibrating the pile and removing the sand directly below the pile with vacuum. The base of the test pile was modified to channel the sand directly below the test pile toward the holes in the base. A large capacity vacuum source was used to remove the sand directly below the pile through two ½-in.-diameter holes in the base. The sand was removed through the pile via two ½-in.-diameter copper tubes that ran from the base, through the center of the pile, and out at the sides of the pile near the top. To keep the sand flowing up the vacuum tubes, compressed air was fed to the base through four ¼-in.-diameter feeder tubes. The feeder tubes ran from the top of the pile, down through the center, and out through the four ¼-in.-diameter holes in the base. The modified pile tip and the plumbing inside the pile, are shown in Figures 2 and 3, respectively.

The installation of the instrumented test pile does not simulate the actual field practice of CIDH pile; disturbance in the surrounding soil and the nonuniformity in density resulting from recompaction should be recognized. Once the instrumented model pile was placed in the soil, the loading arm

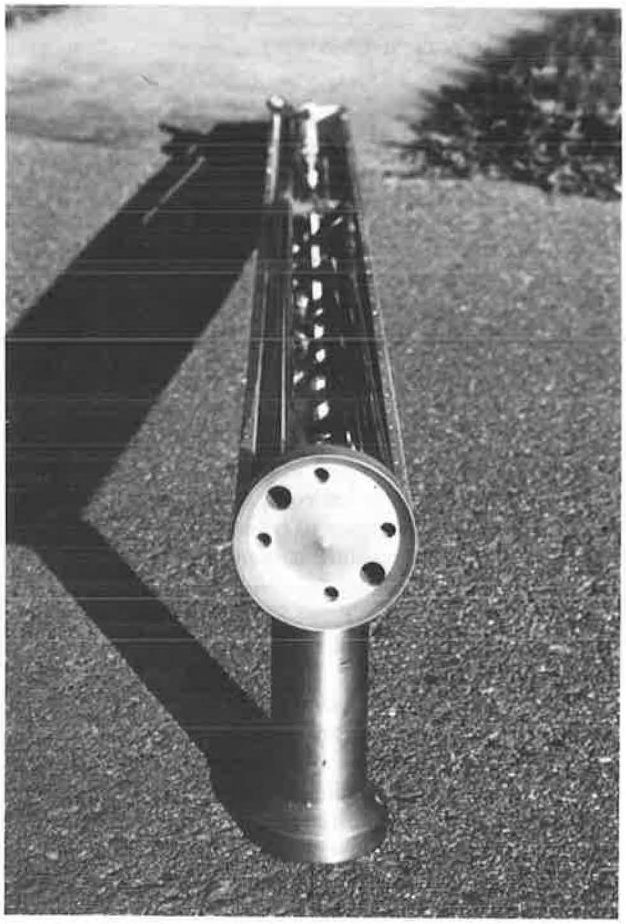

FIGURE 2 Modified pile tip.

was connected to the top of the pile at a predetermined loading height. The photograph in Figure 4 illustrates a typical test setup.

Test Results

A total of 17 tests on sand and 27 tests on silty clay were carried out. Parameters covered in this study were the embedment length (with a slight variation in silty clay soil), the type of loading (monotonic or cyclic), the direction of loading, the sloping nature of the ground, and the distance of the pile from the edge of the slope. Detailed description of each test is given in Tables 2 and 3. The cyclic loading tests were performed on silty clay samples. Different numbers of cycles of low-level loading were applied (Table 3, Tests 29 to 34, inclusive). It was indeed difficult to maintain compaction control when large size test samples were prepared in the model box; thus from sample to sample a substantial amount of scatter existed in the data. However, the results of tests carried out for each individual sample were generally well-behaved and consistent with the loading directions.

One observation that was most apparent during testing was the surface character of the failure zone exhibited in the soil around the pile. A fan-shaped failure zone extending radially from both sides of the pile at 45 degrees or greater to the direction of loading was observed in both level and sloping grounds. A typical ground surface failure pattern can be recognized, as shown in Figure 5.

The typical response of measured lateral load versus displacement in clay embankment and sand embankment can be seen in Figures 6 and 7, respectively. The lateral resistance of the model test piles are given in Table 4. They are recorded as either the maximum lateral load obtained from the load-displacement curves or the lateral load corresponding to approximately 5 degrees of angular rotation of the pile. Because the load cell has a 3,000-lb capacity, a number of tests performed in clay embankments were prematurely terminated at approximately 3,000 lb of lateral load.

When lateral load is applied in the downslope direction on the pile (Figure 8) for both the silty clay and the sand embankments, the placement of the test pile on either the slope or the edge of the slope results in lower lateral resistance than is the case when it is placed with upslope or horizontal loading directions. When the test pile is placed on the edge of a slope and the loading direction is upslope, the resulting load versus displacement curve is approximately the same as the corresponding curve obtained for horizontal loading. Differences, however, can be observed consistently from the test results that show that in clay embankment the lateral resist-

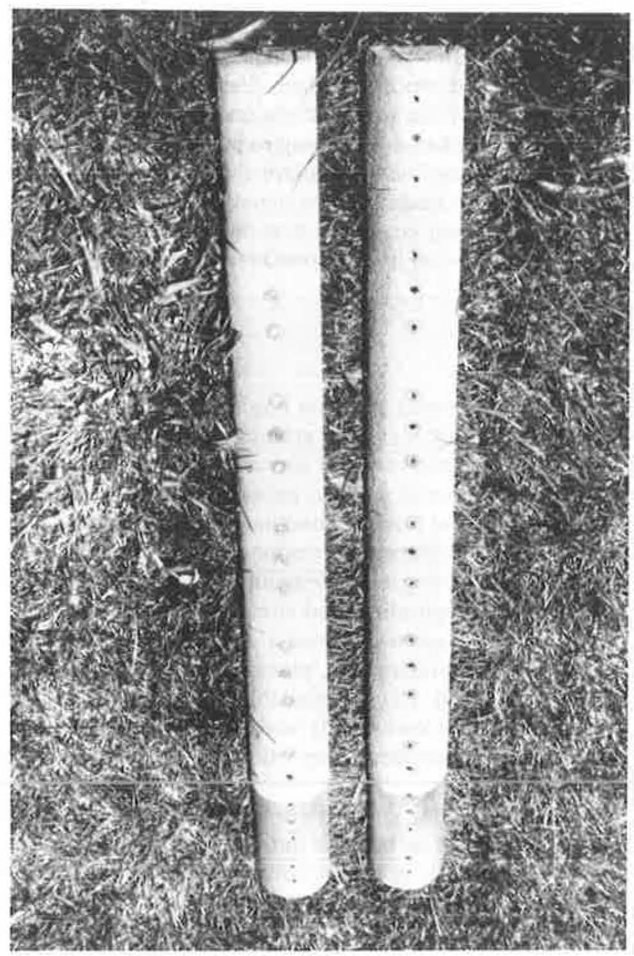

FIGURE 3 Plumbing inside the model test pile.

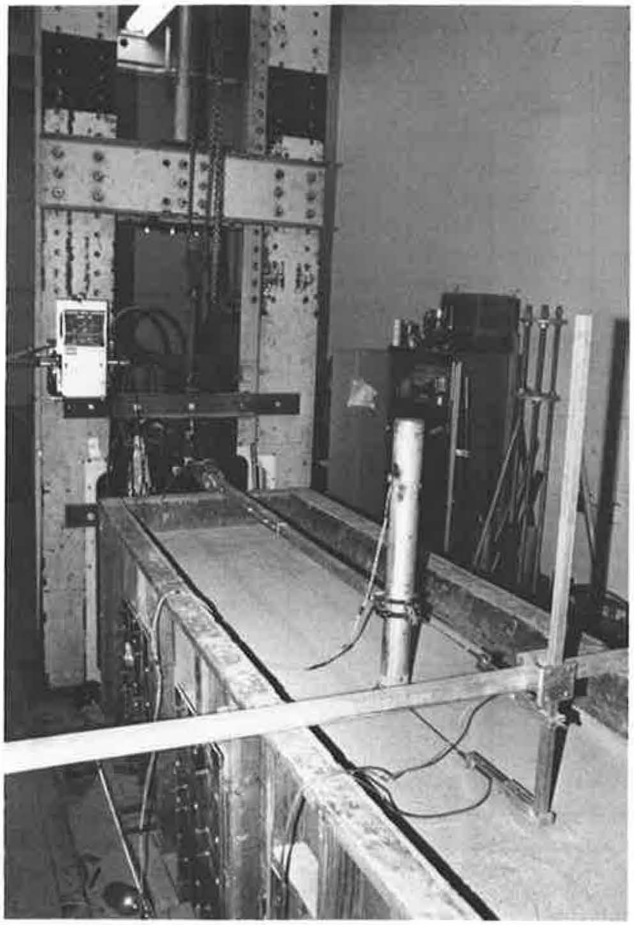

FIGURE 4 Typical test setup.

ance is slightly greater for upslope loading than for horizontal loading, and vice versa for sandy embankment.

For cyclically loaded (push and pull) model pile tests in silty clay (the number of cycles varying from 500 to 2,500 and the low level cyclic loads from approximately 200 to 900 lb at 3 sec/cycle), the results in Figure 9 indicate that the number of loading cycles greater than 500 appears to have little effect on the load-displacement behavior of the model pile. Because the model test condition in the laboratory does not simulate the field cyclic loading environment and does not take into consideration the possible disturbance and weakening of in situ soil, the findings do not agree with the current design concept of reduced pile capacity for cyclic loading applications.

In an effort to develop a three-dimensional picture of the passive earth pressure distributions along the test pile, interface pressure transducers were placed at different locations along the pile circumference from test to test to gather a set of comprehensive data. In Tables 2 and 3, the various θ values represent the angles of transducer locations with respect to the direction of loading: that is, $\theta = 0$ degrees when the transducer is placed in line with the loading direction and $\theta = 90$ degrees when it is placed perpendicular to the loading direction (Figure 8). The data obtained from sandy soil were later normalized and combined to show the radial passive earth pressure distributions against the pile at different depths for various load levels. A typical lateral earth pressure distribution along the depth of a pile in sand under different loading increments is shown in Figure 10. The pressure distributions are nonuniform both circumferentially and longitudinally. In general, the circumferential distribution has its maximum at $\theta = 0$ degrees, and decreases to at-rest pressure at $\theta = 90$ degrees. The longitudinal distribution of pressure

TABLE 2 DESCRIPTION OF TESTS IN CACHE CREEK SAND

Sample#	γ_d (pcf)	Relative Density (%)	Test #	θ_1	θ_2	Slope (%)	Loading Direction	Distance from Edge of Slope or Bin (in)
1	109.8	84.8	1 2 3	0 35 70	N/A N/A N/A	N/A N/A N/A	Horizontal Horizontal Horizontal	52" from edge of bin 76" from edge of bin 107" from edge of bin
2	108.6	80.1	4 5 6	0 0 20	45 45 65	N/A N/A N/A	Horizontal Horizontal Horizontal	47" from edge of bin 78" from edge of bin 108" from edge of bin
3	109.8	84.8	7 8	0 0	45 45	56 N/A	Down Slope Horizontal	Pile 1 in. from edge of slope 108 in. from edge of bin
4	107.9	77.7	9 10	20 20	25 65	59 N/A	Down Slope Horizontal	Pile 1.3 in. from edge of slope 109" from edge of bin
5	109.1	82.4	11 12	0 0	45 45	60 57	Down Slope Up Slope	Pile 1.3 in. from edge of slope Pile 0.8 in. from edge of slope
6	109.0	82.0	13 14	20 0	65 45	58 60	Up Slope Up Slope	Pile 1.8 in. from edge of slope Pile 1.5 in. from edge of slope
7	109.0	82.0	15 16 17	0 20 0	45 65 45	56 56 56	Cross Slope Cross Slope Cross Slope	46" from edge of bin 81" from edge of bin 108" from edge of bin

Note: The height of loading for all tests in sand was 12 inches.
The embedment length for all tests in sand was 32.75 inches.

TABLE 3 DESCRIPTION OF TESTS IN YOLO LOAM

Sample#	W/C (%)	γ_d (pcf)	Test#	θ	Load Height (in)	Embedment Length (in)	Type of Loading	# of Cycles	Loads low/high (lb)	Slope	Loading Direction	Distance From Edge of Slope (in)
2	17.4	115.2	7	0	10.6	33.1	Monotonic	N/A	N/A	Level	Horizontal	40" From edge of bin
			8	20	10.9	33.9						81"
			9	50	10.6	33.9						113"
3	17.2	113.6	10	0	11.4	33.2	Monotonic	N/A	N/A	1:1.5	Down Slope	Pile on edge of slope
			11	0	11.8	33.0				1:1.5	Up	Pile on edge of slope
			12	0	10.8	33.0				Level	Horizontal	Level ground between slopes
4	16.5	109.1	13	0	12.0	31.8	Monotonic	N/A	N/A	1:1.5	Down Slope	Pile on edge of slope
			14	0	11.8	31.9				1:1.5	Up	Pile on edge of slope
			15	0	10.8	33.0				Level	Horizontal	Level ground between slope
5	16.5	111.3	16	0	10.8	33.0	Monotonic	N/A	N/A	1:1.5	Down Slope	Pile ℄:8in down slope
			17	0	10.7	33.1				1:1.5	Up	Pile ℄:8in down slope
			18	0	10.7	33.1				Level	Horizonral	Level ground between slope
6	17.0	111.3	19	0	10.8	26.9	Monotonic	N/A	N/A	1:1.5	Down Slope	Pile on edge of slope
			20	0	10.5	26.0				1:1.5	Up	Pile on edge of slope
			21	0	10.5	27.1				Level Slope	Horizontal	Level ground between slope
7	16.7	112.1	22	0	10.8	33.4	Monotonic	N/A	N/A	1:2	Down Slope	Pile on edge of slope
			23	0	10.4	33.5				Level	Horizontal	Pile ℄:32in behind slope
			24	70	10.5	33.3				Level	Horizontal	Pile ℄:59in behind slope
8	16.6	113.1	26	0	10.6	32.9	Monotonic	N/A	N/A	1:2	Cross Slope	37in From edge of slope
			27	70	10.5	33.0				1:2	Cross Slope	62in From edge of slope
			28	0	10.5	32.9				1:2	Cross Slope	104in From edge of slope
9	15.3	113.7	29	0	11.0	33.0	Cyclic	500	180/880		Horizontal	39in From edge of slope
			30	0	11.0	33.1		1000	200/890		Horizontal	68in From edge of slope
			31	0	11.0	33.1		2500	170/890		Horizontal	104in From edge of slope
10	16.2	111.2	32	0	11.5	33.4	Cyclic	500	5 /450	1:1.5	Down Slope	Pile on edge of slope
			33	0	11.6	32.8		500	30 /860	1:1.5	Up Slope	Pile on edge of slope
			34	0	11.5	32.9		500	50 /810		Horizontal	Level ground between slope

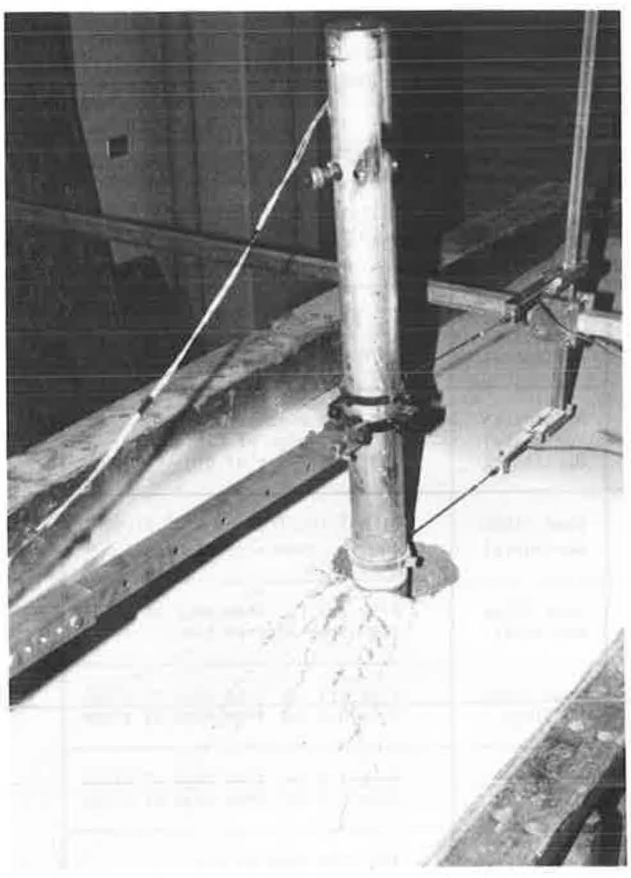

FIGURE 5 Ground surface failure pattern.

is related to both the later displacement and rotation of the pile and the soil depth at the point considered.

CONCLUSIONS

Described in this paper is a laboratory model study of the loading capacity of laterally loaded CIDH piles placed in both level and sloping grounds. Tests were performed in sand as well as in silty clay embankments. Parameters such as the embedment length, the type and direction of loading, the slope of the ground, and the distance from the edge of the slope were included in the study. An instrumented aluminum pipe pile was used to measure the circumferential as well as the longitudinal distributions of lateral earth pressures acting on the pile at different loading levels. Lateral load versus displacement curves for each test were also recorded. Because of difficulties in controlling many of the parameters in testing, particularly the placement densities and moisture contents of the clay soil, large scatter of the test results are evident. Data presented in the paper should therefore be interpreted with caution.

The main purpose of the model study was to develop information concerning the failure pattern and the design capacity of laterally loaded rigid pile. The results presented in this paper can be of help in identifying these items so that a more realistic theoretical formulation of the pile-soil system can be established. Observations pertinent to the overall objective of this investigation can be stated as follows:

1. At ground level, the failure in soil in front of a pile shows a fan-shaped zone originating from the pile at an angle of 45 degrees or greater with the direction of loading.

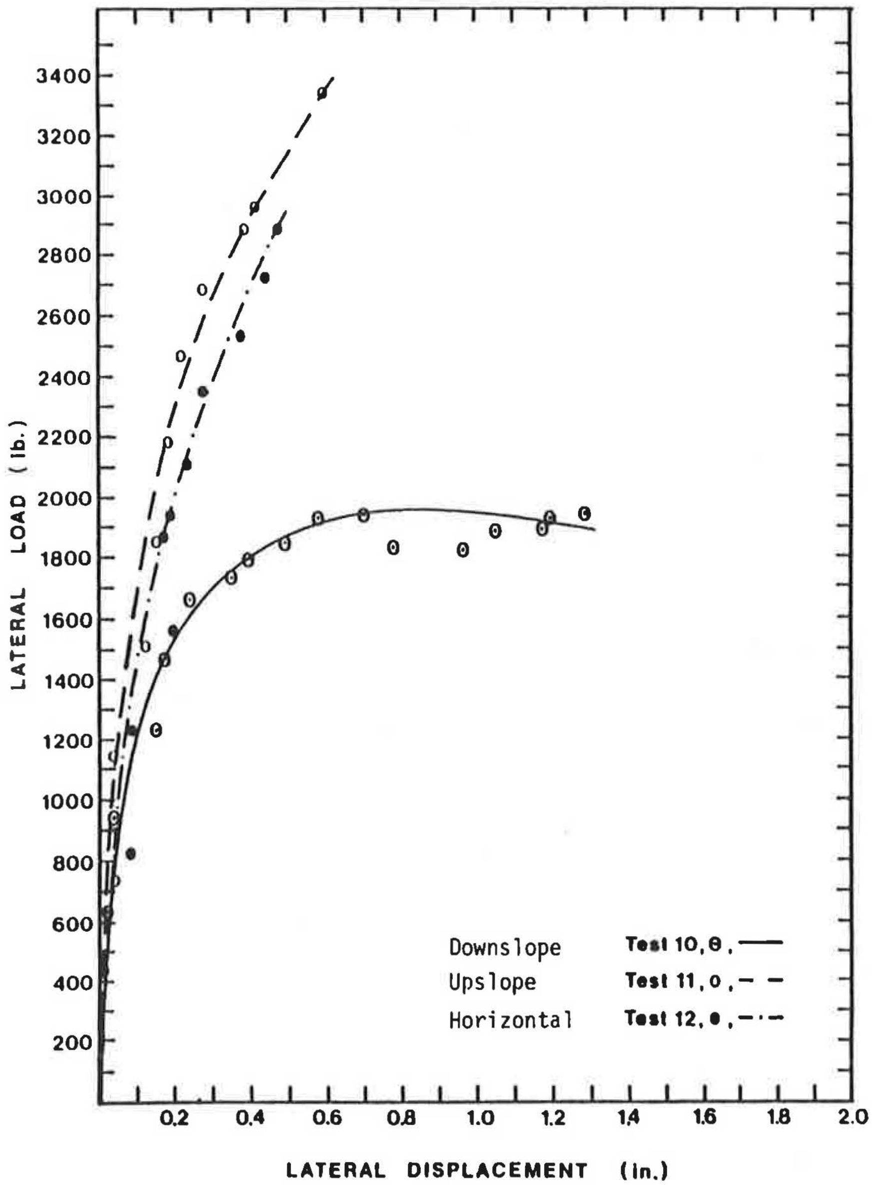

FIGURE 6 Load-deflection at ground line in silty clay.

2. If the pile is placed on a slope and loaded in the downslope direction, its ultimate lateral loading capacity is lower than the capacity produced by a corresponding pile either placed on the slope and loaded in the upslope direction or placed on level ground. Therefore, to be on the safe side, the downslope loading capacity should be used to determine the design lateral resistance for CIDH piles placed on or near an embankment.

3. The passive earth pressure acting on a pile is nonuniform both circumferentially and longitudinally. Furthermore, the magnitudes of earth pressure depend on the movement (displacement or rotation) of the pile with respect to the soil.

ACKNOWLEDGMENTS

The authors are grateful for the support provided by the California Department of Transportation and the Federal Highway Administration.

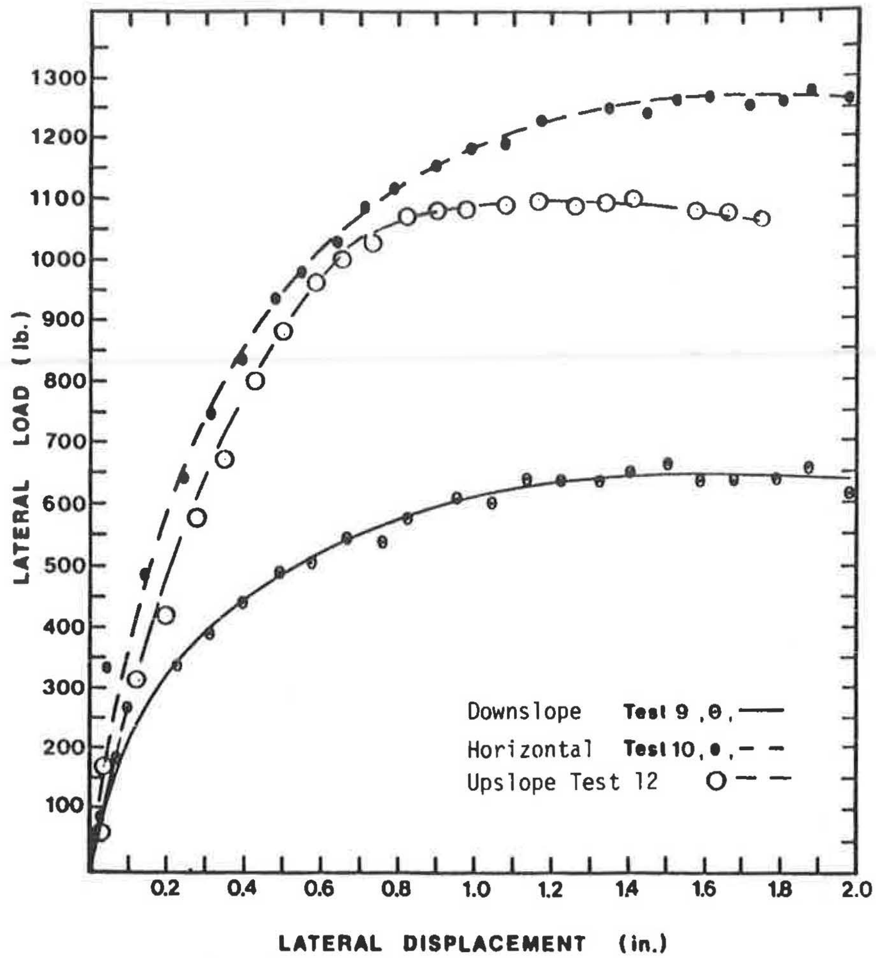

FIGURE 7 Load-deflection at ground line in sand.

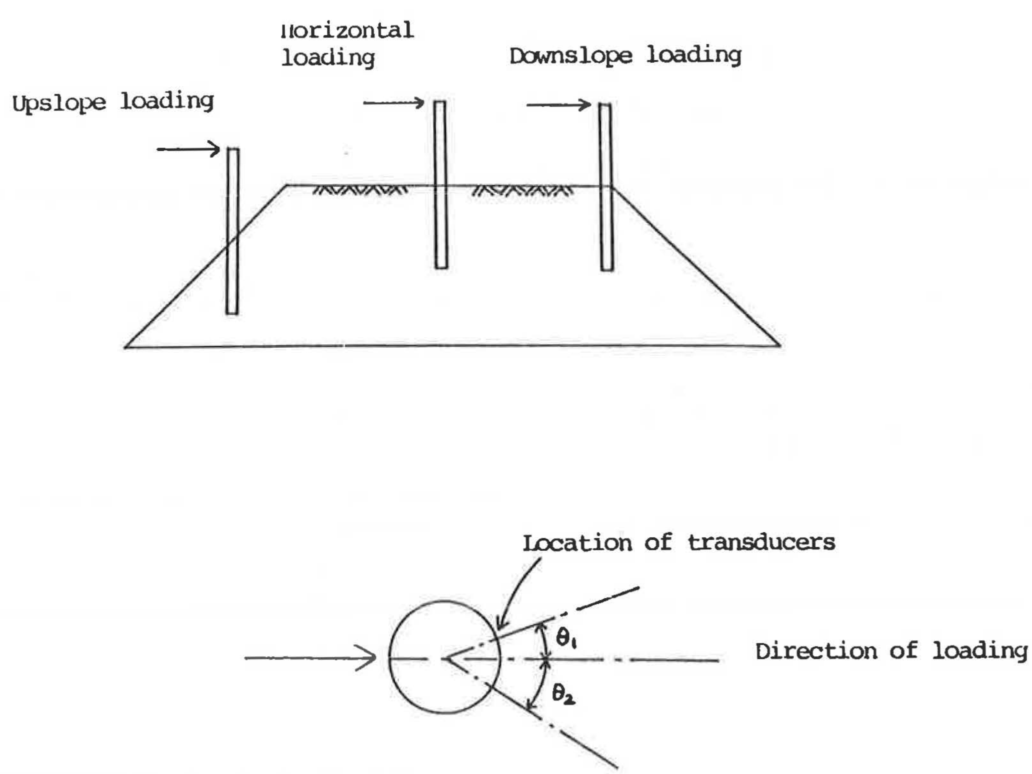

FIGURE 8 Loading direction description.

TABLE 4 LATERAL RESISTANCE OF MODEL TEST PILES

Soil	Test #	Loading direction	Slope (%)	Lateral Resistance (lbs)
Sand	1	Horizontal	N/A	1,040
	2	Horizontal	N/A	1,000
	3	Horizontal	N/A	1,000
	4	Horizontal	N/A	1,040
	5	Horizontal	N/A	970
	6	Horizontal	N/A	960
	7	Downslope	56	450
	8	Horizontal	N/A	1,030
	9	Downslope	59	520
	10	Horizontal	N/A	1,020
	11	Downslope	60	540
	12	Upslope	57	880
	13	Upslope	58	900
	14	Upslope	60	870
	15	Cross-slope	56	970
	16	Cross-slope	56	860
	17	Cross-slope	56	800
Silty Clay	7	Horizontal	N/A	2,650
	8	Horizontal	N/A	2,860
	9	Horizontal	N/A	2,970
	10	Downslope	67	1,900
	11	Upslope	67	2,970
	12	Horizontal	N/A	2,880
	13	Downslope	67	1,480
	14	Upslope	67	2,180
	15	Horizontal	N/A	2,430
	16	Downslope	67	1,390
	17	Upslope	67	3,630
	18	Horizontal	N/A	2,680
	19	Downslope	67	1,050
	20	Upslope	67	2,550
	21	Horizontal	N/A	2,710
	22	Downslope	50	1,820
	23	Horizontal	N/A	2,900
	24	Horizontal	N/A	2,760
	26	Cross-slope	50	2,460
	27	Cross-slope	50	2,550
	28	Cross-slope	50	2,880
	29*	Horizontal	N/A	3,020
	30*	Horizontal	N/A	2,930
	31*	Horizontal	N/A	2,920
	32*	Downslope	67	1,260
	33*	Upslope	67	2,520
	34*	Horizontal	N/A	3,110

* indicates cyclic loading tests

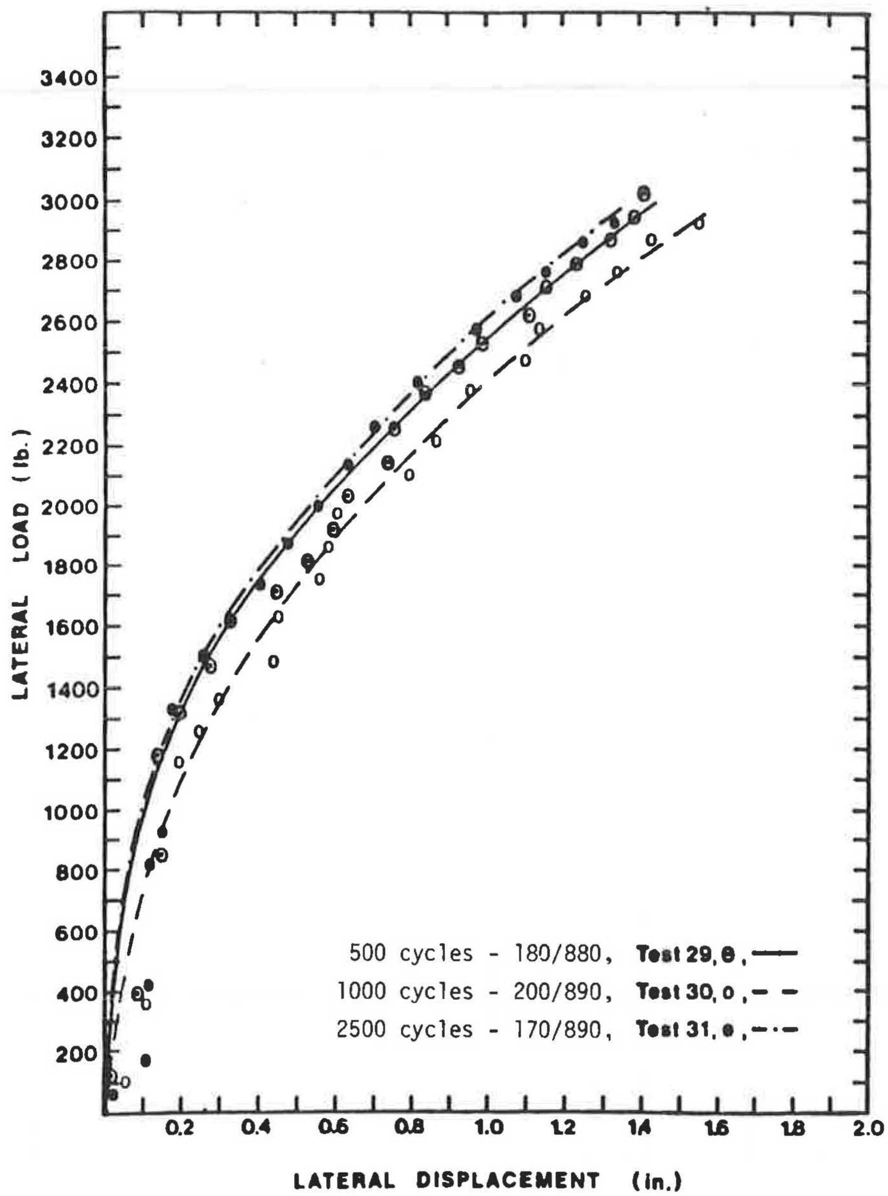

FIGURE 9 Load-deflection at ground line in silty clay—cyclic loading.

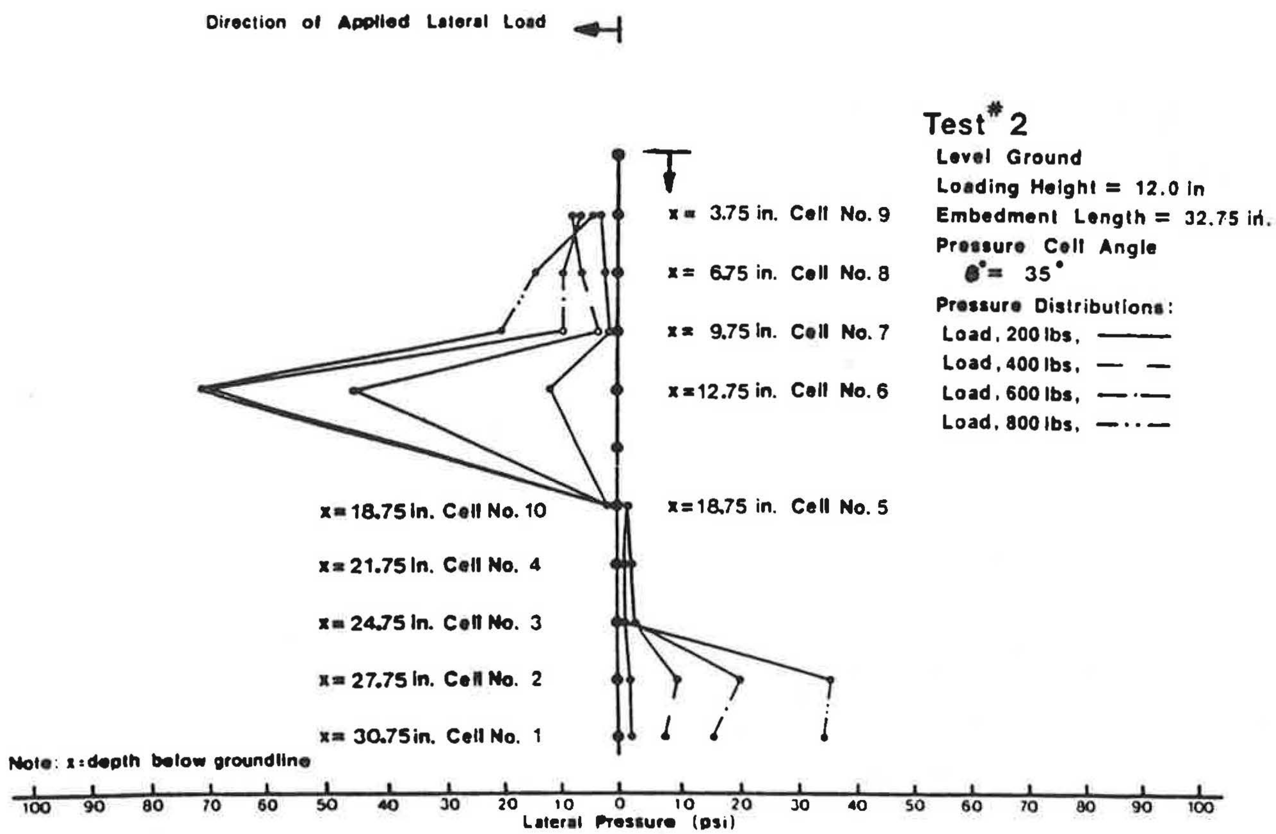

FIGURE 10 Relationship between lateral pressure and depth in sand.

REFERENCES

1. D. L. Ivey. Theory, *Resistance of a Drilled Shaft Footing to Overturning Loads*. Texas Transportation Institute, Texas A&M University, Research Department 105-1, College Station, Feb. 1968.
2. D. L. Ivey and W.A. Dunlap. *Design Procedure Compared to Full-Scale Tests of Drilled Shaft Footings*. Texas Transportation Institute, Texas A&M University, Research Department 105-3, Feb. 1970.
3. D. L. Ivey, K. J. Koch, and C. F. Raba. *Resistance of a Drilled Shaft Footing to Overturning Loads, Model Tests, and Correlation with Theory*. Texas Transportation Institute, Texas A&M University, Research Department 105-2, College Station, July 1968.
4. V. R. Kasch, H. M. Coyle, R. E. Bartoskewitz, and W. G. Sarver. *Lateral Load Test of a Drilled Shaft in Clay*. Texas Transportation Institute, Texas A&M University, Research Department 211-1, College Station, Nov. 1977.
5. B. B. Broms. Lateral Resistance of Piles in Cohesionless Soils. *Journal of Soil Mechanics and Foundation Division*, ASCE, Vol. 90, SM3, 1964.
6. L. C. Reese, W. R. Cox, and F. D. Koop. *Analysis of Laterally Loaded Piles in Sand*. Offshore Technology Conference Paper 2080, Houston, Tex., May 1974.
7. B. B. Broms. Lateral Resistance of Piles in Cohesive Soils. *Journal of Soil Mechanics and Foundation Division*, ASCE, Vol. 90, SM3, 1964.
8. L. C. Reese. *Discussion of Soil Modulus for Laterally Loaded Piles by B. McClelland and J. A. Focht*, ASCE, Vol. 123, 1958.
9. H. Matlock. *Correlations for Design of Laterally Loaded Piles in Soft Clay*. Offshore Technology Conference, Paper No. 1204, Houston, Texas, April, 1970.
10. C. O. Hays, C.O., J. L. Davidson, E. M. Hagan, and R. R. Ristano. *Drilled Shaft Foundation for Highway Sign Structures*. Engineering and Industrial Experiment Station, University of Florida, Research Department D647F, Dec. 1974.
11. D. L. Ivey, and L. Hawkins. Signboard Footings to Resist Wind Loads. *Civil Engineering*, Vol. 36, No. 12, Dec. 1966.
12. J. L. Davidson, C. O. Hays, and E. M. Hagan, Jr. Design of Drilled Shafts Supporting Highway Sign. In *Transportation Research Record 616*, TRB, National Research Council, Washington, D.C., 1976, pp. 62–66.
13. R. L. Lytton. *Design Charts for Minor Service Structure Foundations*. Texas Transportation Institute, Texas A&M University, Research Department 506-IF, Sept. 1971.
14. J. R. Seiler. Effect of Depth of Embedment on Pole Stability. *Wood Preserving News*, Vol. 10, No. 11, Nov. 1932.
15. J. Б. Hansen. *The Ultimate Resistance of Rigid Piles Against Transversal Forces*. The Danish Geotechnical Institute Bulletin, No. 12, Copenhagen, Denmark, 1961.
16. M. W. Bierschwale, H. M. Coyle, and R. E. Bartoskewitz. *Field Tests and Design Procedure for Laterally Loaded Drilled Shafts in Clay*. Texas Transportation Institute, Texas A&M University, Research Department 211-3F, Jan. 1981.
17. G. L. Holloway, H. M. Coyle, R. E. Bartoskewitz, and W. G. Sarver. *Field Test and Preliminary Design Method for Lateral Loaded Drilled Shafts in Clay*. Texas Transportation Institute, Texas A&M University, Research Department 211-2, Sept. 1978.
18. W. L. Shilts, L. D. Graves, and G. G. Driscoll. A Report of Field and Laboratory Tests on the Stability of Posts Against Lateral Loads. In *Proc., 2nd International Conference on Soil Mechanics and Foundation Engineering*, Vol. 5, Rotterdam, The Netherlands, 1948.
19. N. F. Ismael, and T. W. Klym. *Behavior of Rigid Piers in Layered Cohesive Soil*. ASCE, Vol. 104, GTB, Aug. 1978.
20. L. C. Reese. *Design and Construction of Drilled Shafts*. ASCE, Vol. 104, GTI, Jan. 1978.
21. W. V. Wright, H. M. Coyle, R. E. Bartoskewitz, and L. J. Milberger. *New Retaining Wall Design Criteria Based on Lateral Earth Pressure Measurements*. TTI, Texas A&M University, Research Department 169-4F, Aug. 1975.
22. E. Czerniak. Resistance to Overturning of Single Short Piles. *Journal of the Structural Division*, ASCE, Vol. 83, No. ST2, March 1957.

Publication of this paper sponsored by Committee on Subsurface Soil-Structure Interaction.